ARTICLE NO. 79-1552R

Calculation of Pressures on Bodies at Low Angles of Attack in Supersonic Flow

F. R. DeJarnette* and C. P. Ford†
North Carolina State University, Raleigh, N. C.
and
D. E. Young‡
Naval Surface Weapons Center, Dahlgren, Va.

An empirical relation is developed for calculating the pressures over blunted noses. This relation is matched with a new and improved second-order shock-expansion method to calculate approximate surface pressure distributions over blunted and pointed axisymmetric bodies at incidence. Modifications and extensions to the basic second-order shock-expansion method include 1) a new method for locating the position where the second-order shock-expansion method is matched with the blunt-nose pressure relation, 2) an "exact" method for calculating the pressure gradient around a corner, 3) a new expression for calculating pressures around pointed cones at incidence, and 4) a new method for calculating angle-of-attack solutions. The method was found to predict the overexpansion near the juncture of sphere-cones at Mach numbers as low as 1.5. Results were found to compare well with experimental data and exact flowfield computations on blunted cones with and without flares at all Mach numbers greater than 1.5 and angles of attack up to 15 deg. The simplicity and efficiency of the computer program make it attractive for preliminary design applications.

Nomenclature

a = distance from body to streamline A
A = parameter defined by Eq. (8)
B = function defined by Eq. (4)
C_A = axial-force coefficient
C_D = drag coefficient
C_m = pitching-moment coefficient
C_N = normal-force coefficient
C_p = pressure coefficient $= 2(p-p_\infty)/(\rho_\infty V_\infty^2)$
C_1, C_2 = characteristic coordinates
D = parameter defined by Eq. (9)
F = function defined by Eq. (34)
G = function defined by Eq. (17)
K = unified similarity parameter, Eq. (44)
l = body length, calibers
M = Mach number
n = coordinate normal to body, calibers
p = static pressure, dyn/cm^2
p_t = total pressure at stagnation point, dyn/cm^2
r = radius of body of revolution, calibers
R = body radius of curvature, calibers
S = coordinate along a body meridian, calibers
V = velocity, cm/s
x = coordinate along body axis, calibers
α = angle of attack, deg and rad
β = $(M_\infty^2 - 1)^{1/2}$
γ = ratio of specific heats (1.4 for air)
Γ = $[2/(\gamma M_\infty^2)][\partial^2(p/p_\infty)/\partial\alpha^2]_{\phi=0,\alpha=0}$
δ = flow inclination angle and cone angle, deg
Δ = $[2/(\gamma M_\infty^2)][\partial^2(p/p_\infty)/\partial\alpha^2]_{\phi=\pi/2,\alpha=0}$
ϵ = crossflow angle, deg
η = function defined by Eq. (2)
θ = shock wave angle, deg
λ = function defined by Eq. (5)
Λ = $[1/(\gamma M_\infty^2)][\partial(p/p_\infty)/\partial\alpha]_{\phi=0,\alpha=0}$
μ = Mach angle = $\sin^{-1}(1/M)$
ν = Prandtl-Meyer expansion angle, deg
ρ = density, g/cm^3
ϕ = circumferential angle (0 deg in windward plane, 180 deg in leeward plane)
Ω = ratio of cross-sectional area of streamtube to that at $M=1$, see Eq. (6)

Superscripts

$( )^*$ = evaluated where $M=1$

Subscripts

0 = surface streamline
0_1 = beginning of the expansion on the surface
1 = condition at start of Prandtl-Meyer expansion
2 = condition at end of Prandtl-Meyer expansion
∞ = freestream conditions
A = streamline off the surface
c = quantities evaluated for pointed cone tangent to the body
equiv = refers to equivalent cone quantities
m = matching point
MNewt = modified Newtonian value
N = nose
Newt = Newtonian value
SB = slender body approximation
stag = stagnation value

Presented as Paper 79-1552 at the AIAA 12th Fluid and Plasmadynamics Conference, Williamsburg, Va., July 23-25, 1979; submitted Sept. 11, 1979; revision received June 12, 1980.

Index category: Supersonic and Hypersonic Flow.

*Professor, Mechanical and Aerospace Engineering. Associate Fellow AIAA.

†Assistant Professor; presently with Brunswick Corp. Member AIAA.

‡Engineering Trainee, Aeromechanics Branch. Student Member AIAA.

Introduction

PRELIMINARY design of new configurations requires methods which will calculate the aerodynamic characteristics efficiently and be reasonably accurate. Wind tunnel and ballistic range tests are generally too expensive and time consuming for the number of configurations normally

considered. Numerical methods which calculate the entire inviscid flowfield require computational times and storage too large to use in design optimization processes. Therefore, computer programs which combine analytical techniques and semiempirical methods appear to be most advantageous for preliminary design purposes. This paper presents an approximate method for calculating the surface pressure distribution on axisymmetric bodies at angles of attack from 0 to 15 deg and all Mach numbers greater than 1.5.

Moore and Swanson[1] modified Van Dyke's second-order perturbation method to calculate surface pressures over both pointed and blunted bodies of revolution. This method was shown to yield results which compared well with experimental data for angles of attack up to 15 deg and Mach numbers less than about 3. Jackson et al.[2] modified the second-order shock-expansion method[3] for blunt-nosed bodies at small angles of attack. This method predicted surface pressures which compared reasonably well with experimental data on blunted cones with and without flares at Mach numbers from 2.3 to 4.63 and angles of attack up to 12 deg. Of particular importance was the fact that their method predicted some of the overexpansion near the juncture of sphere-cones at Mach numbers greater than about 2.0. However, below Mach 2, the pressure prediction near the juncture was poor. In addition, the pressures calculated on the conical afterbodies at angles of attack did not approach the correct limit.

This paper describes new modifications and extensions made to the second-order shock-expansion method which make it more accurate than Jackson's method and applicable to Mach numbers greater than 1.5 and angles of attack up to about 15 deg. Although there is some overlap, the present method is intended to complement that of Moore and Swanson.[1] Some of the modifications and results presented in this paper are described in more detail in Ref. 4; an earlier version of this paper appears in Ref. 5.

Background

Before the new modifications are described, the basic second-order shock-expansion method at zero angle of attack will be reviewed.

Second-Order Shock-Expansion Method

The basic second-order shock-expansion method was developed by Syvertson and Dennis[3] for pointed bodies near $\alpha=0$ deg at supersonic speeds. In order to apply this method, the actual body is replaced by a tangent body which is a series of conical frustums tangent to the actual body at a selected number of positions. The pressure along the initial cone is constant, but the pressure drops discontinuously across the juncture of the initial cone and the following conical frustum. This pressure drop can be calculated from the standard Prandtl-Meyer expansion. In the generalized (first-order) shock-expansion method, the pressure along each conical frustum is taken to be constant, but it follows an exponential variation in the second-order shock-expansion method. This exponential pressure variation is made to satisfy three boundary conditions. First, the pressure p_2 just after the corner of two conical frustums (Fig. 1) is that obtained from the Prandtl-Meyer expansion. The second boundary condition is that the pressure gradient $(\partial p/\partial S)_2$ at this same position is set equal to that obtained from an approximate expression developed by Syvertson and Dennis.[3] For the third boundary condition, the pressure on this conical frustum is forced to approach the pointed-cone pressure, p_c, as if it was infinitely long. Thus, the pressure distribution along a conical frustum is given by

$$p=p_c-(p_c-p_2)e^{-\eta} \tag{1}$$

where

$$\eta=\left(\frac{\partial p}{\partial S}\right)_2\frac{(x-x_2)}{(p_c-p_2)\cos\delta_2} \tag{2}$$

The pressure gradient just downstream of the corner is determined from the approximate expression

$$\left(\frac{\partial p}{\partial S}\right)_2-\lambda_2\left(\frac{\partial\delta}{\partial S}\right)_2 = \frac{B_2}{r}\left(\frac{\Omega_1}{\Omega_2}\sin\delta_1-\sin\delta_2\right)+\frac{B_2}{B_1}\frac{\Omega_1}{\Omega_2}\left[\left(\frac{\partial p}{\partial S}\right)_1-\lambda_1\left(\frac{\partial\delta}{\partial S}\right)_1\right] \tag{3}$$

where

$$B=\gamma pM^2/2(M^2-1) \tag{4}$$

$$\lambda=2\gamma p/\sin 2\mu \tag{5}$$

$$\Omega=\frac{1}{M}\left[\frac{1+M^2(\gamma-1)/2}{(\gamma+1)/2}\right]^{\frac{(\gamma+1)}{2(\gamma-1}} \tag{6}$$

Note that $(-\partial\delta/\partial S)$ is the curvature of the surface which is zero on conical frustums, and Ω is the one-dimensional area ratio. For the first corner after the initial cone, $(\partial p/\partial S)_1=0$ since the pressure is constant on the initial cone. The pressure gradient ahead of subsequent conical frustums is obtained from the derivative of Eq. (1).

The pressure obtained from Eq. (1) is used only at the position where the conical frustum is tangent to the actual body. If the conical frustum has a negative cone angle, Ref. 3 suggests using $p_c=p_\infty$ on that segment. Reference 3 also gives an expression for the pressure gradient downstream of a sharp concave corner such as a flare. One restriction on the method described here is that the pressure gradient just downstream of a corner $(\partial p/\partial S)_2$ must have the same sign as the pressure difference (p_c-p_2); otherwise, Eq. (1) will not yield the third boundary condition that $p=p_c$ as $x\to\infty$.

Modifications by Jackson et al.

The original second-order shock-expansion method was developed for pointed noses with attached shock waves. Jackson et al.[2] modified it for blunt-nosed bodies by using the modified Newtonian pressure distribution up to a "matching point" and then applying the second-order shock-expansion method downstream of that point. They found that the best matching point corresponded to the point on the blunted nose where the body slope is the same as the maximum wedge angle for an attached shock wave. A tangent body is used to replace the actual body downstream of the matching point. The pressure on the first conical frustum tangent to the matching point is taken to be constant and equal to the modified Newtonian pressure for that body angle. The pressure distribution downstream of the first conical frustum is calculated by the original second-order shock-expansion method.[3] For those conical frustums which have the sign of the initial pressure gradient $(\partial p/\partial S)_2$ opposite from the sign of (p_c-p_2), the pressure is taken to be

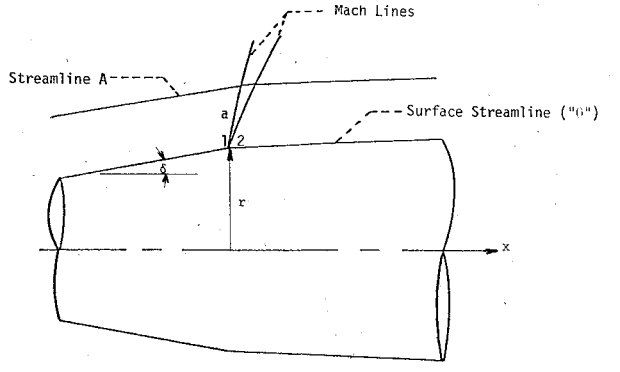

Fig. 1 Flow about a convex corner on a body of revolution.

p_2. This makes the technique on those conical frustums identical to the generalized shock-expansion method. Reference 2 found this condition to occur on the nose of spherically blunted cones at $M_\infty \gtrsim 3.0$ and also on the flares of blunted cone-flare bodies. The modifications made for bodies at an angle of attack are discussed in a following section.

Results for blunted cones and blunted cones with flares were found to compare well with experimental data for $M_\infty \geq 3.0$. For the range $1.5 \leq M_\infty \lesssim 3$, the method predicted only part of the pressure overexpansion at the shoulder. However, this inaccuracy was found to have only a small effect on the force and moment coefficients.

New Method for Calculating Surface Pressures

The approach used here is somewhat similar to that of Jackson et al.[2] An empirically determined equation is used to calculate the pressures over blunted noses around to a matching point. Then, an improved second-order shock-expansion method is applied from the matching point downstream. For bodies with pointed noses and attached shock waves, the pointed-cone pressure is used at the nose, and then the improved second-order shock-expansion method is used to calculate the pressures downstream of the nose. However, modifications and extensions were made to the method of Jackson et al[2] for both blunted- and pointed-nosed bodies in order to increase the accuracy of the method and extend the range of applicability to all Mach numbers greater than about 1.5 and for angles of attack up to about 15 deg. The following five changes were made:

1) A new empirical equation was developed to replace the modified Newtonian expression for calculating pressures on blunted noses.

2) A new matching point was determined for matching the nose pressures with the improved second-order shock-expansion method on blunt-nosed bodies.

3) An exact expression for the pressure gradient downstream of a corner is developed to replace the approximate expression given by Eq. (3).

4) For bodies at an angle of attack, a new expression is determined for calculating pointed-cone pressures at incidence, which replaces the tangent cone method generally used.

5) A new technique is developed for calculating pressures on bodies at incidence.

Pressure Distribution on Blunted Noses

The modified Newtonian theory gives reasonably accurate pressure predictions on blunt noses at hypersonic speeds. However, when this theory was compared with exact inviscid flowfield calculations[6] over a sphere at $M_\infty \geq 3.5$, differences were observed. In the region about 45 deg from the stagnation point, modified Newtonian pressures are too high, whereas they are too low near the shoulder. At Mach numbers near 1.5, modified Newtonian theory predicts pressures higher than experimental[2] and calculated[7] flowfield results over a sphere. In order to start the second-order shock-expansion method, accurate values of pressure and pressure gradient must be known at the matching point. Therefore, the following empirical equation was developed to calculate both pressures and pressure gradients on blunt-nosed bodies from the stagnation point around to the matching point:

$$C_p = C_{P_{stag}} (1 - D\cos^A \delta) \tag{7}$$

The parameters A and D are functions of M_∞. They were determined at several values of M_∞ by finding the values which made Eq. (7) fit the results given in Refs. 2 and 6 the best in a least squares sense. Then, these values were curve fit by the following equations:

$$A = 2.6054749 - 0.4659981\, M_\infty + 0.09303905\, M_\infty^2 - 0.00817329\, M_\infty^3 + 0.00026447\, M_\infty^4 \tag{8}$$

$$D = 1.570367 - 0.565058\, M_\infty + 0.2071167\, M_\infty^2 - 0.0341656\, M_\infty^3 + 0.00210593\, M_\infty^4 \quad (\text{for } 1.5 \leq M_\infty \leq 3.8)$$

$$D = 1.0081057 - 0.0132323\, M_\infty + 0.00164956 M_\infty^2 - 0.00006797\, M_\infty^3 \quad (\text{for } 3.8 < M_\infty \leq 10) \tag{9}$$

Equation (7) was found to give more accurate predictions of both pressures and pressure gradients on spheres than the modified Newtonian theory. Figure 2 shows the comparison on a sphere at $M_\infty = 1.9$. Additional comparisons have been made up to $M_\infty = 10$ with good results. Note that Eq. (7) reduces to the modified Newtonian expression where $A = 2$ and $D = 1$. Equations (8) and (9) give $1.72 < A < 2.09$ and $0.97 < D < 1.08$.

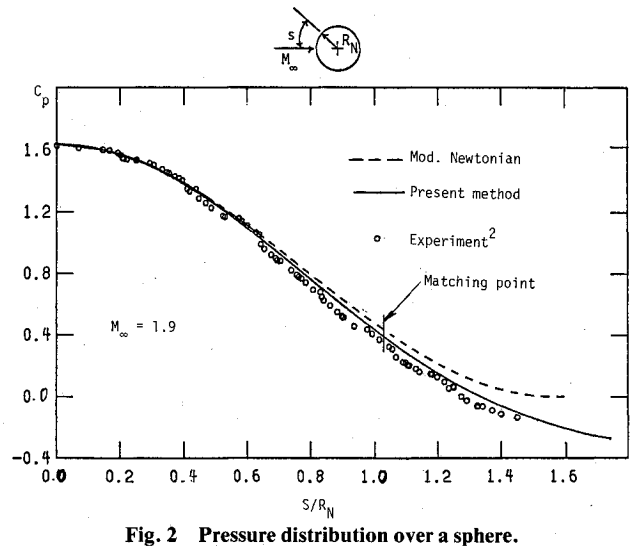

Fig. 2 Pressure distribution over a sphere.

New Matching Point on Blunted Noses

The location of the point used to match the nose pressure distribution to the second-order shock-expansion method has a large effect on the accuracy of predicting the overexpansion on blunted cones at the lower supersonic Mach numbers. As previously mentioned, Jackson et al.[2] used the position where the body slope is the same as the maximum wedge angle for an attached shock wave. They found that this location predicted part of the overexpansion at the shoulder. The results compared well with experimental data at $2.30 \leq M_\infty \leq 4.63$, where the overexpansion is small, but the comparison was poor at $M_\infty = 1.5$, where the overexpansion is large.

Jackson et al.[2] assumed the pressure gradient to be zero on the first conical frustum at the matching point. However, both Eqs. (3) and (27) show that whenever the body curvature $(-\partial\delta/\partial S)$ is discontinuous, then the pressure gradient is discontinuous, even if the body slope is continuous. For a blunted nose, the body radius of curvature just forward of the matching point is R_1, whereas the radius of curvature on the conical frustum is infinite, and hence $(\partial\delta/\partial S)_2 = 0$. Thus, at the matching point, the pressure gradient at the beginning of the first conical frustum is given by both Eqs. (3) and (27) as

$$\left(\frac{\partial p}{\partial S}\right)_2 = \left(\frac{\partial p}{\partial S}\right)_1 + \frac{\lambda_1}{R_1} \tag{10}$$

and since the slope is continuous, $p_2 = p_1$. The pressure and pressure gradient at the matching point (subscript 1) come from Eq. (7).

The pressure distribution downstream of the matching point can now be calculated by the second-order shock-

expansion method. Equation (10) gives the pressure gradient on the first conical frustum (which is tangent to the nose at the matching point). A tangent body is then transcribed about the remaining body, and the technique described previously can be applied. Note, however, that the pressure gradient at each corner is calculated from the "exact" expression given by Eq. (27).

The location of the matching point on a sphere was determined for several values of M_∞ by finding the position which produced the smallest deviation, in a least squares sense, of the pressures calculated by the present method from the results given in Refs. 2 and 6. At each value of M_∞, the location of the matching point was converted to the local Mach number (there) M_m by using the isentropic relation between Mach number and p/p_t. These values were then used to curve fit the matching Mach number (M_m) to M_∞, and the following relation was obtained:

$$M_m = 0.724667 + 0.373147\,M_\infty - 0.06498948M_\infty^2 + 0.00640026\,M_\infty^3 - 0.00025873\,M_\infty^4 \quad (\text{for } 1.5 \le M_\infty < 10) \tag{11}$$

This equation gives M_m varying monotonically from about 1.16 at $M_\infty = 1.5$ up to about 1.77 at $M_\infty = 10$. Figure 2 shows the pressure distribution over a sphere at $M_\infty = 1.9$. In order to obtain good accuracy from the second-order shock-expansion method, about 40 conical frustums were used to approximate the sphere from the matching point to the shoulder. At $M_\infty = 1.9$, the matching Mach number given by Eq. (11) is 1.24. However, when additional calculations were made by increasing and decreasing this value of M_m by 0.05, the results were indistinguishable for the scale of Fig. 2. The sensitivity of the downstream solution to the matching Mach number is very small for $M_\infty > 1.9$. This is due to the accuracy of Eq. (7) in predicting the pressures over the sphere. References 4 and 5 found the sensitivity to be much greater because modified Newtonian pressures were used back to the matching point. However, the sensitivity of the matching Mach number on the downstream solution is much greater for $1.5 \le M_\infty < 1.9$.

Derivation of Exact Pressure Gradient Downstream of a Corner for $\alpha = 0$ deg

As previously mentioned, the pressure gradient given by Eq. (3) is only approximate. Therefore, an "exact" expression is derived here to compare with it. Although an "exact" expression is derived in Ref. 8, it is not in a form comparable to Eq. (3). For the following analysis, refer to Fig. 1 for the nomenclature and geometry. Consider a surface streamtube as it passes around a corner. The stream surface (A) is close to the body surface, and the distance along a Mach line between the two stream surfaces is a (where a is very small). As the flow turns around the corner, the distance a will increase because M increases, and hence the distance between the stream surfaces will increase.

Define C_1 and C_2 as characteristic coordinates and S and n as coordinates along and normal to a streamline. At a corner only the C_1 family of characteristics (left-running characteristics) is present. The analytical development here is based on two equations from the method of characteristics[3]:

$$\frac{\partial p}{\partial C_1} = \cos\mu\left(\frac{\partial p}{\partial S} - \lambda\frac{\partial \delta}{\partial S}\right) \tag{12}$$

and

$$\frac{\partial \delta}{\partial C_1} = \frac{-\sin\mu\sin\delta}{r} - \frac{\cos\mu}{\lambda}\left[\frac{\partial p}{\partial S} - \lambda\frac{\partial \delta}{\partial S}\right] \tag{13}$$

Multiply Eq. (12) by dS_0 and apply it on the surface to get

$$\frac{\partial p}{\partial C_1}\,dS_0 = \cos\mu_0\left(\frac{\partial p}{\partial S} - \lambda\frac{\partial \delta}{\partial S}\right)dS_0 = \cos\mu_0(dp_0 - \lambda_0 d\delta_0) \tag{14}$$

where the subscript 0 refers to the surface streamline. Since $\partial p/\partial C_1$ is finite, and the distance around the corner (dS_0) is zero, the left side of Eq. (14) is zero, and the result is the Prandtl-Meyer expression

$$-d\nu_0 = dp_0/\lambda_0 = d\delta_0 \tag{15}$$

which integrates to

$$\nu_0 - \nu_{0_1} = \delta_{0_1} - \delta_0 \tag{16}$$

The subscript 0_1 refers to the beginning of the expansion on the surface.

Define the function G by

$$G = \int \frac{dp}{\lambda} - \delta \tag{17}$$

Then, using Eqs. (12) and (13), the partial derivatives of G are

$$\frac{\partial G}{\partial S} = \frac{1}{\lambda}\frac{\partial p}{\partial S} - \frac{\partial \delta}{\partial S} = \frac{1}{\lambda\cos\mu}\frac{\partial p}{\partial C_1} \tag{18}$$

$$\frac{\partial G}{\partial C_1} = \frac{1}{\lambda}\frac{\partial p}{\partial C_1} - \frac{\partial \delta}{\partial C_1} = 2\cos\mu\frac{\partial G}{\partial S} + \frac{\sin\mu\sin\delta}{r} \tag{19}$$

Note that since $\lambda = \lambda(p, p_t)$, Eq. (19) neglects $\partial p_t/\partial C_1$ which is zero for conical noses and generally negligible for blunt noses.

Now, consider a streamline off the surface, denoted as streamline A in Fig. 1. The coordinate C_1 has the length a along a Mach line, and a changes from one Mach line to another in the expansion fan. If a^* is the length corresponding to $M = 1$, then a can be related to Ω, the ratio of the one-dimensional cross-sectional area of the streamtube to that at $M = 1$, as follows:

$$\frac{a}{a^*} = \frac{2\pi r a}{2\pi r a^*} = \frac{\Omega}{\sin\mu} \tag{20}$$

Note that the thickness of the streamtube is ($a\sin\mu$), and thus the cross-sectional area of the streamtube is ($2\pi r a\sin\mu$). Along a Mach line, the first two terms of the Taylor series expansion about the surface give

$$G_A = G_0 + \left(\frac{\partial G}{\partial C_1}\right)_0 a + \ldots \tag{21}$$

Take the partial derivative of this equation with respect to distance along streamline A to get

$$\frac{\partial G_A}{\partial S_A} = \frac{\partial G_0}{\partial S_A} + \frac{\partial}{\partial S_A}\left[\left(\frac{\partial G}{\partial C_1}\right)_0 a\right] + \ldots \tag{22}$$

From Appendix A of Ref. 4, the distance dS_A is related to $d\delta_0$ by

$$\frac{dS_A}{d\delta_0} = -a\left(\frac{\gamma+1}{2}\right)\frac{M_0^3}{(M_0^2 - 1)} \tag{23}$$

Now, Eq. (15) can be used to obtain

$$\frac{\partial G_0}{\partial S_A} = \frac{dG_0}{d\delta_0}\frac{d\delta_0}{dS_A} = \left(\frac{1}{\lambda}\frac{dp}{d\delta} - 1\right)_0 \frac{d\delta_0}{dS_A} = 0 \tag{24}$$

The Taylor series expansion for $\partial G/\partial S$ about the surface gives

$$\left(\frac{\partial G}{\partial S}\right)_A = \left(\frac{\partial G}{\partial S}\right)_0 + \left[\frac{\partial}{\partial C_1}\left(\frac{\partial G}{\partial S}\right)\right]_0 a + \ldots \tag{25}$$

Now, substitute Eqs. (23-25) into Eq. (22), divide the result by a^*, and take the limit as $a^* \to 0$. This gives

$$\left(\frac{\partial G}{\partial S}\right)_0 = \frac{d\delta_0}{dS_A} a^* \frac{d}{d\delta_0}\left[\frac{\partial G}{\partial C_1}\frac{a}{a^*}\right] \tag{26}$$

Finally, substitute Eqs. (19), (20), and (23) into Eq. (26) to get

$$-\left(\frac{\partial G}{\partial S}\right)_0 \left(\frac{\gamma+1}{2}\right)\frac{\Omega_0 M_0^4}{(M_0^2-1)} = \frac{d}{d\delta_0}\left[\Omega\left(\sqrt{M_0^2-1}\cdot 2\left(\frac{\partial G}{\partial S}\right)_0 + \frac{\sin\delta_0}{r}\right)\right] \tag{27}$$

This equation can be integrated numerically around the corner with the Prandtl-Meyer expansion to determine $(\partial G/\partial S)$, and by using Eq. (18), $(\partial p/\partial S)_0$ is determined from $(\partial G/\partial S)_0$.

It should be noted that if the left side of Eq. (27) is set equal to zero, the right side can be integrated, and the result is the same approximate expression obtained by Syvertson and Dennis [see Eq. (3)]. Equation (27) is also the same as the equation derived in a different manner in Ref. 4.

Figure 3 compares the pressure gradient parameter

$$\frac{r}{p_\infty}\frac{\partial p}{\partial C_1} = \frac{r}{p_\infty}\cos\mu\frac{\partial p}{\partial S}$$

calculated from the approximate method [Eq. (3)] with the exact method [Eq. (27)]. The pressure gradient is presented for different deflection angles of a biconic with an initial 40-deg half-angle cone at $M_\infty = 2.5$ and 5. The approximate method differs by as much as 40% from the exact method. It is also worth noting that negative pressure gradients are obtained for $M_\infty = 5$, whereas only positive values are obtained at $M_\infty = 2.5$.

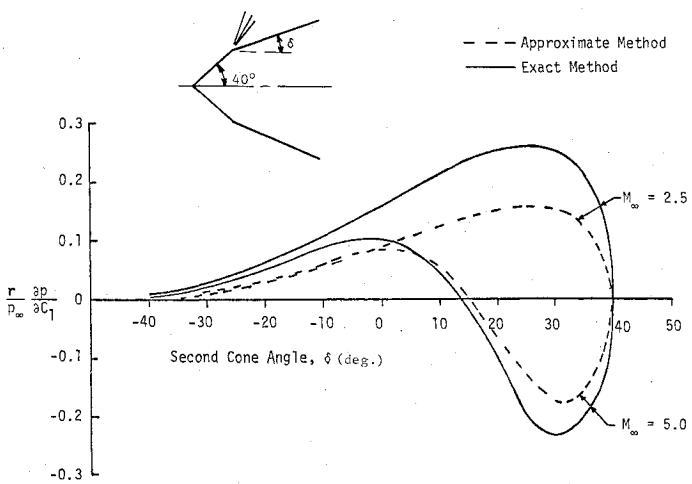

Fig. 3 Pressure gradient at corner of biconics, initial cone angle = 40 deg.

Pressure Distribution for $\alpha > 0$ deg

An accurate calculation of surface pressures on bodies of revolution at $\alpha > 0$ deg is much more complicated than that for the body at $\alpha = 0$ deg. At $\alpha = 0$ deg, the meridian lines on the surface are also surface streamlines. However, at incidence, the streamlines wrap around the body and no longer follow the meridian lines. If the shape of a streamline can be determined approximately, then an equivalent body of revolution can be generated for that streamline, and the method described for $\alpha = 0$ deg can be used to calculate the pressure distribution along this equivalent body of revolution representing the streamline. Several streamlines must be used in order to get the circumferential pressure distribution along the actual body.

Jackson et al.[2] assumed that the surface streamlines in the windward and leeward planes of symmetry could be approximated by the body shape obtained by transforming the body-axis coordinates into wind-axis coordinates. This transformation is obtained by rotating the body-axis coordinate system in the plane of symmetry clockwise through the angle α with the center of rotation at the center of the spherical cap. The windward and leeward streamlines are transformed into the equivalent bodies of revolution represented by the body coordinates in the wind-axis system. On the other hand, the streamline for $\phi = 90$ deg is approximated by the body-axis coordinates of a meridian of the true body shape. The equivalent body of revolution for this streamline is, therefore, the same as the true body at $\alpha = 0$ deg. A similar technique was used in Ref. 4 for determining the streamlines beyond the spherical nose.

An approach different from those previously described is used here. The pressure coefficient is written as

$$C_P = \underset{\alpha=0}{C_P}(x) + \sin 2\alpha\cos\phi\Lambda(x) + \sin^2\alpha[\cos^2\phi\Gamma(x) + \sin^2\phi\Delta(x)]/2 \tag{28}$$

where $\Delta(x)$, $\Gamma(x)$ and $\Lambda(x)$ are loading functions defined in the nomenclature. Note that Λ is the same as that used in Ref. 3. The form of Eq. (28) is the same in both α and ϕ as that given by modified Newtonian and slender body theories. The loading functions are calculated in the same fashion as Eq. (1) in that the distribution along a conical frustum is

$$\Lambda = \Lambda_c - (\Lambda_c - \Lambda_2)e^{-\eta} \tag{29}$$

and similarly for Δ and Γ. Expressions for the cone and blunted-nose values of the loading functions can be determined from the pointed-cone pressure distribution at $\alpha > 0$ (see following section) and modified Newtonian theory, respectively. Expressions are needed, however, to determine their values downstream of a corner.

Syvertson and Dennis[3] used the Prandtl-Meyer expansion to find

$$\frac{\partial(p_2/p_\infty)}{\partial\alpha} = \frac{\lambda_2}{\lambda_1}\frac{\partial(p_1/p_\infty)}{\partial\alpha} \tag{30}$$

This equation gives

$$\Lambda_2 = \lambda_2\Lambda_1/\lambda_1 \tag{31}$$

and the derivative of Eq. (30) gives

$$\Delta_2 = \lambda_2\Delta_1/\lambda_1 \tag{32}$$

and

$$\Gamma_2 = [\Gamma_1 + 2\gamma p_\infty M_\infty^2\Lambda_1^2(F_2 - F_1)/\lambda_1]\lambda_2/\lambda_1 \tag{33}$$

where

$$F=[(\gamma+1)M^4/2-2M^2+2](M^2-1)^{-3/2} \quad (34)$$

In deriving Eq. (32), use was made of the fact that Eq. (28) gives

$$\left[\frac{\partial(p/p_\infty)}{\partial\alpha}\right]_{\phi=\pi/2,\alpha=0}=0 \quad (35)$$

Since the streamlines make an angle ϵ with body meridian lines and $\epsilon\sim\sin\phi\sin\alpha$, then the fact that streamlines are not body meridians does not affect Eq. (32) because ϵ always occurs as $\cos\epsilon$. For Eq. (33), the isentropic relation between p and M was used to show that

$$\frac{\partial\lambda}{\partial\alpha}=F\frac{\partial p}{\partial\alpha}$$

The pressure distribution for $\alpha>0$ is determined from Eq. (28). The loading functions Δ,Γ, and Λ are calculated on each conical frustum along with $p_{\alpha=0}$. Equation (28) has the advantage of giving C_p, at any $\alpha<15$ deg and ϕ once the three loading functions are calculated. In addition, force and moment coefficients can be calculated easily from Eq. (28).

Pointed-Cone Pressure Distribution at $\alpha>0$ deg

In the application of the second-order shock-expansion method at $\alpha>0$ deg, the pointed-cone pressure as a function of ϕ is needed. Reference 2 used the tangent-cone pressure, whereas Ref. 4 found a more accurate expression to be

$$p_c=p_{c_{\alpha=0}}+p_{\text{M Newt}}-p_{\text{M Newt},\alpha=0} \quad (36)$$

This equation gives the change in cone pressure with α as the change in modified Newtonian pressure with α. Equation (36) was found to give more accurate results than the tangent-cone method. The results also compared well with experimental data on the windward side, but the comparison was not very good on the leeward side. A more accurate expression is derived here.

It was found that for cones at the lower supersonic Mach numbers and small angles of attack, slender body theory predicted the change in pressure due to α very well. However, slender body theory does not predict accurate $\alpha=0$ deg pressures. Therefore, the exact cone solution at $\alpha=0$ deg is used, and the pressure coefficient is given by

$$C_p=C_{p_{\alpha=0}}+\Delta C_p \quad (37)$$

where slender body theory[10] gives

$$\Delta C_{p_{SB}}=4\alpha\tan\delta\cos\phi+(1-4\sin^2\phi)\alpha^2 \quad (38)$$

On the other hand, Newtonian theory gives

$$\Delta C_{P_{\text{Newt}}}=2(\sin^2\delta_{\text{equiv}}-\sin^2\delta)$$

$$=\sin2\alpha\sin2\delta\cos\phi+\sin^2\alpha\cos^2\delta(2-2\tan^2\delta-2\sin^2\phi) \quad (39)$$

where

$$\sin\delta_{\text{equiv}}=\cos\alpha\sin\delta+\sin\alpha\cos\delta\cos\phi \quad (40)$$

By comparing Eqs. (38) and (39), it is observed that within the accuracy of slender body theory, the functional form of each term involving α, δ, and ϕ is the same; only the constants differ. Therefore, an expression which reduces to Eq. (38) for small α and δ at $M_\infty=\sqrt{2}$ and to Eq. (39) for large M_∞ is

$$\Delta C_p=\sin2\alpha\sin2\delta\cos\phi$$

$$+\sin^2\alpha\cos^2\delta[(2-1/\beta)(1-\tan^2\delta)-(2+2/\beta)\sin^2\phi] \quad (41)$$

When this equation is used in Eq. (37), an accurate prediction of the pointed-cone pressure at $\alpha>0$ deg is obtained. An accurate value of the cone pressure and shock angle at $\alpha=0$ can be calculated by the equations in Ref. 11 if the angles are replaced by the sine of the angle and if M_∞ is replaced by

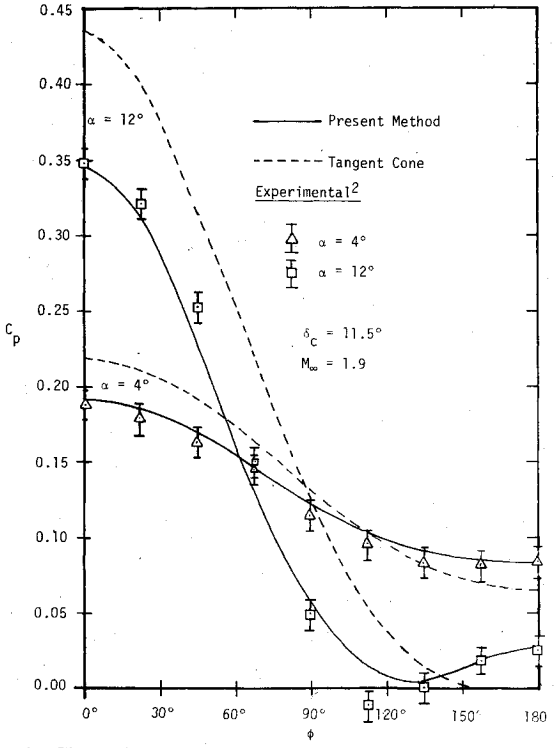

Fig. 4 Circumferential pressure distribution around a pointed cone.

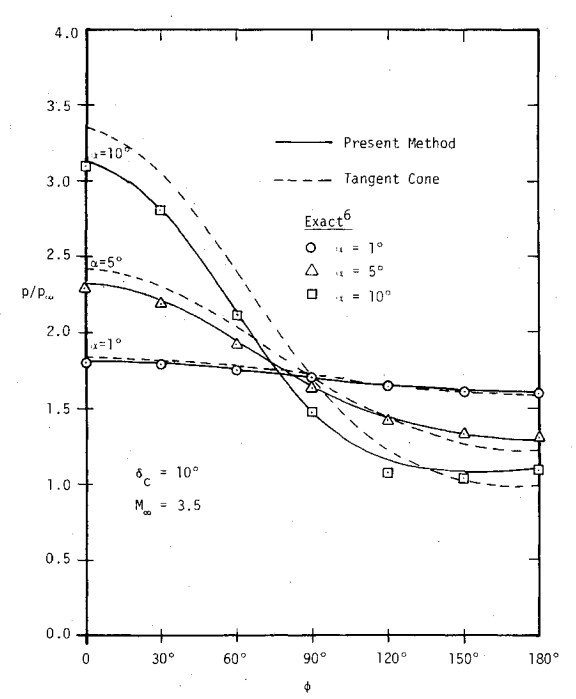

Fig. 5 Circumferential pressure distribution around a pointed cone.

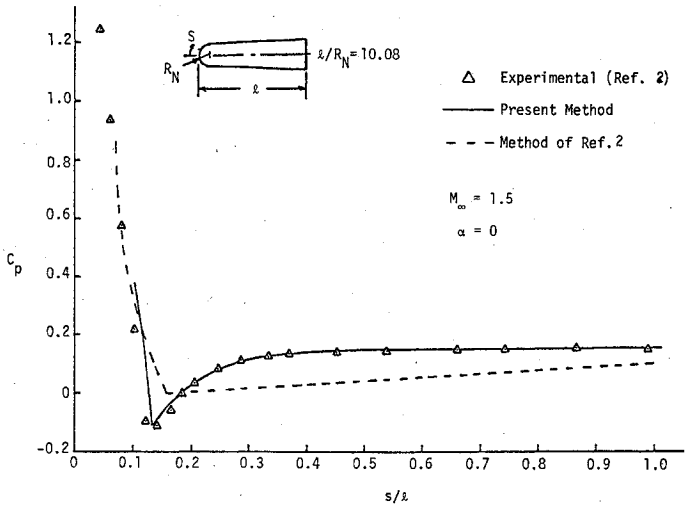

Fig. 6 Pressure distribution on spherically blunted 11.5 -deg cone.

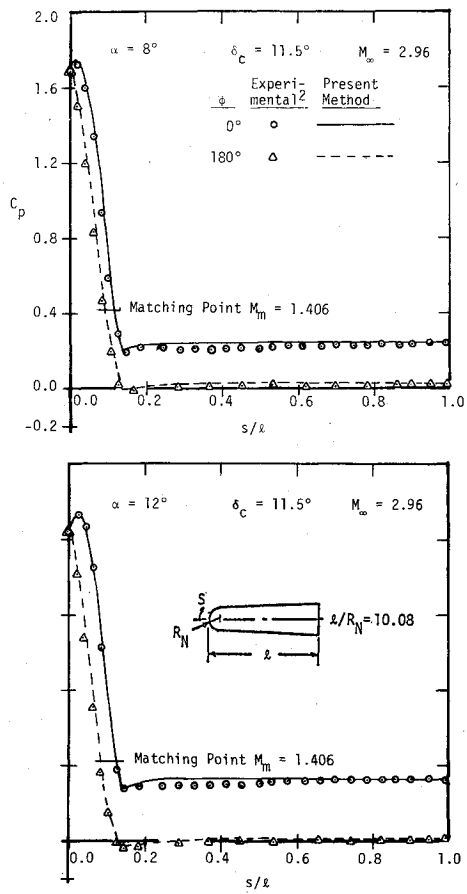

Fig. 7 Pressure distribution on blunted cone.

$\sqrt{M_\infty^2 - 1}$ in the equation for C_p. These replacements give the shock-wave angle as

$$\sin\theta = \sin\delta_c \left[\frac{\gamma+1}{2} + \frac{1}{M_\infty^2 \sin^2\delta_c} \right]^{1/2} \tag{42}$$

and the pressure coefficient by

$$C_{p_{\alpha=0}} = \sin^2\delta_c \left[1 + \frac{(\gamma+1)K^2+2}{(\gamma-1)K^2+2} \ln\left(\frac{\gamma+1}{2} + \frac{1}{K^2} \right) \right] \tag{43}$$

where

$$K^2 = (M_\infty^2 - 1)\sin^2\delta_c \tag{44}$$

Equations (42) and (43) compare very well with the exact cone solution for $1.05 \le M_\infty < \infty$ at all cone angles except near the shock detachment angle. Equation (44) defines the unified supersonic-hypersonic similarity parameter for Eq. (43) so that it will approach the result from linearized theory as $K \to 0$. Since shock waves are not used in linearized theory, Eq. (42) gives better accuracy using the hypersonic similarity parameter to obtain the shock-wave angle.

To test the accuracy of Eq. (41), comparisons were made with the tangent-cone method, exact numerical calculations,[6] and experimental data.[2] Figure 4 gives the circumferential variation of the pressure coefficient around a pointed 11.5-deg cone at $M_\infty = 1.9$ with $\alpha = 4$ and 12 deg. The vertical lines through the experimental data points indicate the range of uncertainty in the experimental results. Figure 5 gives the pressure distribution around a pointed 10-deg cone at $M_\infty = 3.5$ with $\alpha = 1$, 5, and 10 deg. These figures show that the present method compares well with experimental and exact numerical calculations, and it is much more accurate than the tangent-cone method. Since Jackson et al.[2] used the tangent-cone method, this explains why their calculations did not approach the experimental data on conical afterbodies at incidence. At hypersonic Mach numbers, the present method was found to be even more accurate, and the results tend to approach tangent-cone pressures near $M_\infty = 10$.

Results and Discussion

Figure 6 illustrates the capability of the present method to predict the pressure overexpansion near the shoulder of a spherically blunted 11.5-deg cone at $M_\infty = 1.5$ and zero incidence. It also shows that the method of Jackson et al.[2] predicts only part of the overexpansion at the lower supersonic Mach numbers. Figure 7 shows the pressure distribution in the windward ($\phi = 0$ deg) and leeward ($\phi = 180$ deg) planes of the spherically blunted 11.5-deg cone at $M_\infty = 2.96$ and $\alpha = 8$ and 12 deg. This figure shows that the present method compares well with the experimental data. It also illustrates that the pressure overexpansion decreases as the Mach

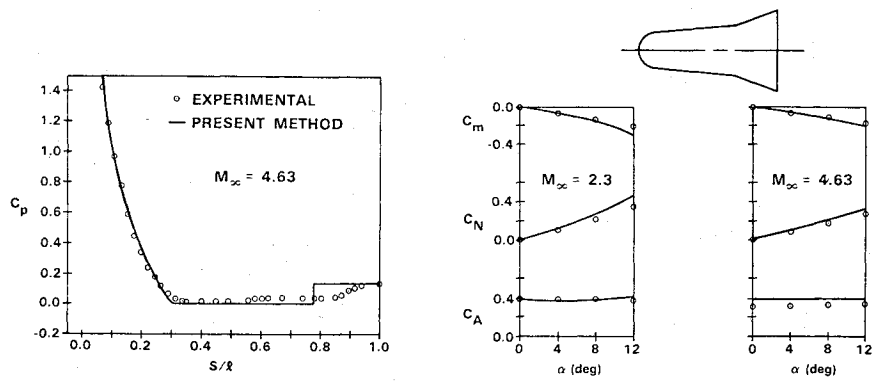

Fig. 8 Aerodynamic characteristics of blunted cone-flare body.

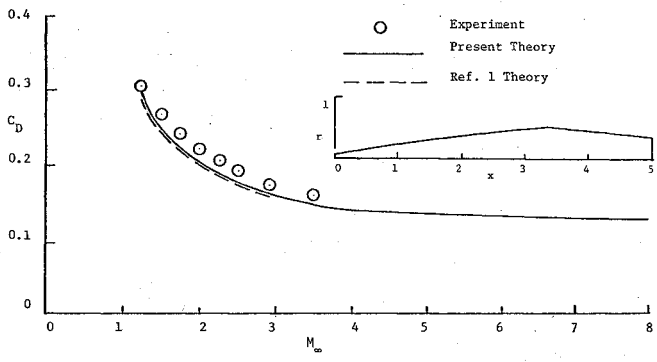

Fig. 9 Drag coefficient for 30-mm projectile.

number increases. For $M_\infty \gtrsim 3.5$, it was found that, in the application of the second-order shock-expansion method, the sign of the initial pressure gradient $(\partial p/\partial S)_2$ on conical frustums was opposite to that of $(p_c - p_2)$ over most of the region downstream of the matching point. When this condition occurred, the pressure on that conical frustum was taken to be p_2, and the present method is identical to the generalized (first-order) shock-expansion method. Thus, at $M_\infty \gtrsim 3.5$, the present method gives results very close to that of Jackson et al.[2]

Figure 8 compares the present method with experimental data[2] for a blunted 2.75 -deg cone with an 18 -deg flare. One part of the figure shows the pressure distribution at $M_\infty = 4.63$ and $\alpha = 0$ deg. Note that there is no pressure overexpansion near the sphere-cone juncture for this case. Also, it appears that flow separation occurred at the beginning of the flare, which caused the experimental data to drop significantly below the theory. Figure 8 also gives results for the pitching-moment, normal-force, and axial-force coefficients as a function of α for $M_\infty = 2.3$ and 4.63. The experimental data[2] represent results calculated from the experimental pressures, not actual force and moment data. The present method compares well with the experimental data, and at these Mach numbers, the method of Jackson et al.[2] gives results close to the present method.

Figure 9 compares the drag coefficient calculated from the present method and that of Ref. 1 with experimental data for a 30-mm projectile with a truncated nose. The drag includes pressure drag, skin-friction drag, and base drag. The skin-friction and base drags used here are the same as those used in Ref. 1. This figure shows that the present method predicts drag coefficients very close to those of Ref. 1 and the experimental data for $1.25 \leq M_\infty < 3$. The method used in Ref. 1 is a modified Van Dyke second-order perturbation method. Therefore, it is limited to $M_\infty \lesssim 3$.

The computer program used for the results presented in this paper is relatively fast, requiring less than 15 seconds of CPU time for a typical case on an IBM 370/165 computer.

Conclusions

1) The empirical equation developed for predicting pressures over blunted noses is more accurate than modified Newtonian theory.

2) The pressure overexpansion near the shoulder of blunted cones at low supersonic speeds can be predicted accurately by the present method. This is due to the technique developed for matching the nose pressure distribution with the improved second-order shock-expansion method.

3) The exact method developed for calculating the pressure gradient downstream of a corner gives results which differ by as much as 40% from the approximate relation normally used in the second-order shock-expansion method.

4) The new equation developed for calculating pressures on pointed cones at incidence is much more accurate than the tangent-cone method. It also increases the accuracy of the improved second-order shock-expansion method used in the calculations at an angle of attack.

5) The present method is well suited for making engineering calculations on bodies of revolution at $M_\infty \gtrsim 1.5$ and angles of attack up to about 15 deg.

Acknowledgments

This research was supported by the Naval Surface Weapons Center, Dahlgren, Va., under Contract No. N60921-77-C-A066. The authors wish to thank Drs. Frank G. Moore, Leroy Devan, and John Sun of the Naval Surface Weapons Center for their assistance and advice in the development of this work. Appreciation is also extended to Ms. Joyce Pollard for typing the manuscript.

References

[1] Moore, F.G. and Swanson, R.C., Jr., "Aerodynamics of Tactical Weapons to Mach Number 3 and Angle of Attack 15°," Part I - Theory and Application, NSWC/DL TR-3584, Feb. 1977, and Part II - Computer Program and Usage, NSWC/DL TR-3600, March 1977.

[2] Jackson, C.M., Jr., Sawyer, W.C., and Smith, R.S., "A Method for Determining Surface Pressure on Blunt Bodies of Revolution at Small Angles of Attack in Supersonic Flow," NASA TN D-4865, 1968.

[3] Syvertson, C.A. and Dennis, D.H., "A Second-Order Shock-Expansion Method Applicable to Bodies of Revolution Near Zero Lift," NACA Report 1328, 1957.

[4] DeJarnette, F.R. and Jones, K.M., "Development of a Computer Program to Calculate Aerodynamic Characteristics of Bodies and Wing-Body Combinations," NSWC/DL TR-3829, April 1978.

[5] DeJarnette, F.R. and Ford, C.P., "A New Method for Calculating Surface Pressures on Bodies at an Angle of Attack in Supersonic Flow," *Proceedings of the 11th Navy Symposium on Aeroballistics,* Vol. II, Aug. 22-24, 1978, pp. 199-231.

[6] Morrison, A.M., Solomon, J.M., Ciment, M., and Ferguson, R.E., "Handbook of Inviscid Sphere-Cone Flowfields and Pressure Distributions," Vols. I and II, NSWC/WOL/TR 75-45, Dec. 1975.

[7] Hsieh, T., "Flowfield Study About a Hemispherical Cylinder in Transonic and Low Supersonic Mach Number Range," AIAA Paper 75-83, 1975.

[8] Johannsen, N.H. and Meyer, R.E., "Axially-Symmetrical Supersonic Flow Near the Center of an Expansion," *Aeronautical Quarterly,* Vol. II, Aug. 1950, pp. 127-142.

[9] Hayes, W.D. and Probstein, R.F., *Hypersonic Flow Theory,* Vol. I, *Inviscid Flows,* 2nd Ed., Academic Press, New York, 1966.

[10] Liepmann, H.W. and Roshko, A., *Elements of Gasdynamics,* John Wiley and Sons, Inc., New York, 1957, p. 245.

[11] Rasmussen, M.L., "On Hypersonic Flow Past an Unyawed Cone," *AIAA Journal,* Vol. 5, Aug. 1967, pp. 1495-1497.